

Dear Editor,

We are grateful for receiving your thoughtful feedback. And we thank for the time and effort invested by both the editor and the reviewers in providing constructive suggestions that have significantly contributed to enhancing the quality of this work, particularly in addressing the role of in-cloud HMS formation during our observations, a point highlighted by all three reviewers. We acknowledge that despite the acceptance of our explanations and revisions by two reviewers, Anonymous Referee #3 may still have consideration on this point, alongside other comments. Therefore, please find below our detailed point-to-point responses to the comments from Anonymous Referee #3. The referee's comments are presented in italics, followed by our responses in normal font.

Comment # 1

Given the short lifetime of clouds (approximately 20-30 minutes), it is inherently difficult to rule out the possibility of cloud processing even on days classified as “clear.” Therefore, the evidence for HMS formation occurring solely in aerosols under urban conditions-without any contribution from cloud chemistry-remains limited.

Response: Thanks for the comment. We agree with the reviewer that the contribution of in-cloud HMS formation cannot be completely ruled out during our observations in urban Nanjing. However, as indicated in our previous response, the prevalent presence of temperature inversions (**Figure S3**, attached below) across our urban observations could largely impede the transportation of gas precursors emitted near surface to high altitudes and the descent of chemicals produced in high-altitude clouds to ground level (Wang et al., 2022). Besides, low wind speeds (**Figure S2a**) were observed during our observations. These conditions may suggest that even if HMS were largely formed with cloud droplets, its contribution to near surface aerosol were largely inhibited. Furthermore, days lacking temperature inversions (from December 19th to December 23th, 2023) were associated with negligible cloud water content (**Figure S2f**), which were obtained from MERRA-2 (Modern-Era Retrospective analysis for Research and Applications, Version 2) (Gelaro et al., 2017). And the lower levels of HMS observed in this work compared to other polluted areas such as Northern China (Ma et al., 2020; Wei et al., 2020; Wang et al., 2024) may also suggest the minor contribution from in-cloud formation.

In addition, we attempted to compare the HMS formation rate in cloud water ($P_{HMS, c}$) and aerosol water ($P_{HMS, a}$) in urban Nanjing, despite the potential hindrance to in-cloud HMS formation transport. Global models (Song et al., 2019) have estimated the cloud pH in the winter of Nanjing area to be around 4-5, consistent with winter observations in China (4.1 ± 0.6) (Shah et al., 2020). In our analysis, we utilized the upper value of cloud pH of 5 to estimate $P_{HMS, c}$ under pre-haze and haze conditions, comparing it with $P_{HMS, a}$ (**Table R1**). Despite the tendency for cloud pH to decrease

during haze pollution (Li et al., 2017), it was observed that $P_{HMS, c}$ was 2-5 times lower than $P_{HMS, a}$ in the winter of Nanjing. Nevertheless, it is worth noting that the $P_{HMS, a}$ value of $1.06 \pm 0.64 \times 10^{-2} \mu\text{g m}^{-3} \text{h}^{-1}$ during hazy days can effectively reflect the HMS levels observed in ambient aerosol, furthering indicate the predominate role of aerosol water for HMS formation during temperature inversion. We acknowledged that uncertainties may exist in the calculation of $P_{HMS, c}$ due to reduced precursor concentrations resulting from weak vertical exchange and potential variability associated with cloud pH, thus above information was not included in the Manuscript.

Overall, while we recognize that the HMS formation in cloud layers characterized by persistent dense clouds and extended durations may carry great contributions, in the context of this study, the presence of temperature inversions, low wind speeds, and diminished cloud water content during the winter season in Nanjing suggests that the impact of in-cloud HMS formation on the observed levels of particulate HMS may be insignificant. Further discussion on the role of in-cloud HMS chemistry was expanded in the Manuscript.

Revision in Manuscript:

Page 19, Line 29: “Collectively, this study provided valuable information for the prevalence of HMS and the validation the model-derived outcomes concerning HMS quantification. The work primarily concentrated on particulate HMS formation in aerosol liquid water, highlighting the role of moderate-level ionic strength in atmospheric HMS formation, advocating for their integration into global or regional models to better represent the particulate sulfur chemistry, especially in humid environments. Nevertheless, it is noted that in-cloud HMS chemistry may also contribute to the particulate HMS levels where vertical and high-altitude observations are required to fully understand its significance, thus warranting further investigation.”

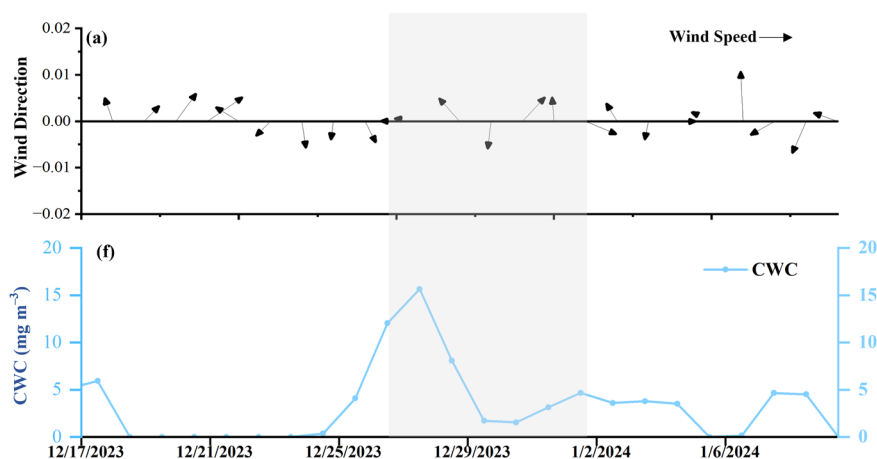


Figure S2. Ancillary atmospheric measurements in urban Nanjing including wind speed and wind direction (a); Time series of the average cloud water content below the planetary boundary layer height over our observation sites (f). Gray shadow indicates the haze period.

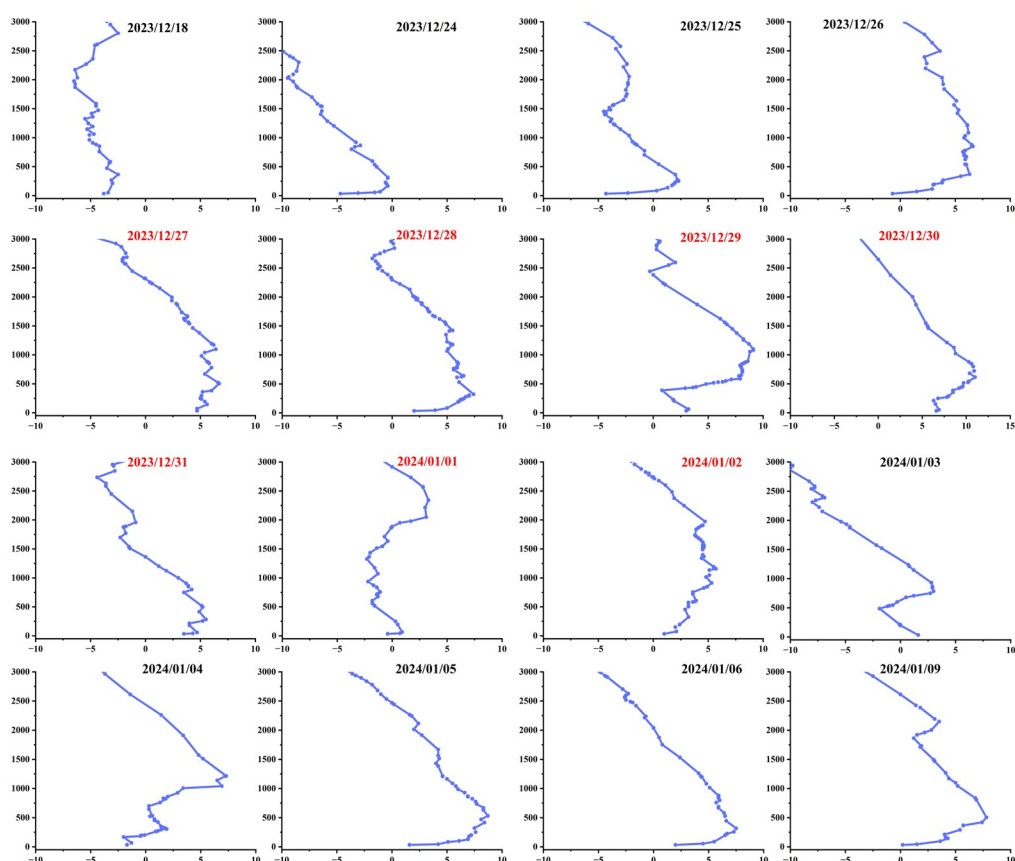


Figure S3. Observed vertical temperature profile at 00 UTC during our observation in Nanjing. The dates of hazy days were marked by red.

Table R1. Summary of $P_{HMS, a}$ and $P_{HMS, a}$ as well as input parameters.

Urban Nanjing				
	Cloud		Aerosol	
	Pre-haze	Haze	Pre-haze	Haze
T (K)	272±2	277±4	272±2	277±4
SO₂ (ppb)	1.99±0.45	2.21±0.69	1.99±0.45	2.21±0.69
HCHO (ppb)	1.91±1.05	5.38 ±1.08	1.91±1.05	5.38 ±1.08
LWC ($\mu\text{g m}^{-3}$)	1.5±2.2 mg m^{-3}	5.12±5.45 mg m^{-3}	22.69±20.65	80.45±38.40
pH	5 ^a	5	5.25±0.42	4.76±0.46
Ionic strength (mol kg^{-1})	10 ⁻⁴ ^b	10 ⁻⁴	12.32±3.19	8.85±1.30
P_{HMS} ($\times 10^{-4} \mu\text{g m}^{-3} \text{h}^{-1}$)	2.56±4.68	20.4±23.3	6.40±6.96	106±64.6

^a This cloud pH was the upper value of global estimation on Nanjing aera (Song et al., 2019).

^b This typical ionic strength value of cloud droplet was given by Herrmann et al. (2015).

Comment # 2

The proposed role of ionic strength in HMS formation is largely based on model calculations. In the current version of the paper, there is no direct observational evidence presented to support the effect of ionic strength.

Response: Thanks for the feedback. It appears that the "model calculation" mentioned likely pertains to our calculated HMS formation rates (P_{HMS}). In this work, these calculated P_{HMS} were compared with observed HMS to carbon dioxide (CO) ratio to highlight the potential role of ionic strength in HMS formation, as elaborated in the **Manuscript (Page 13)**. Initially, considering the low reactivity of HMS, we utilized the ratio of HMS to CO observations (HMS/CO) to better represent the secondary formation of ambient HMS as CO was usually considered to be an inert chemical species during rapid haze formation, with its variation often interpreted as indicative of the diffusion or accumulation of primary pollutants in the shallower boundary layer (Williams et al., 2016). During our study period, enhanced HMS formation was noted during hazy days as evident by the higher HMS/CO ratio (0.51 ± 0.11) (**Figure 2f**, attached below). Additionally, we compared the P_{HMS} calculations with and without the consideration of ionic strength. With the consideration of ionic strength, P_{HMS} calculations exhibited a good correlation with HMS/CO ($R=0.57$) (**Figure S9a**). More importantly, we identified increased HMS formation rates during haze events, with average P_{HMS} of $5.8 \pm 5.9 \times 10^{-3} \mu\text{g m}^{-3} \text{h}^{-1}$ compared to that during the clean periods ($4.5 \pm 8.4 \times 10^{-4} \mu\text{g m}^{-3} \text{h}^{-1}$), aligning well with the HMS/CO ratio (**Figure 2f**). Noteworthy, when the ionic strength effect in aerosol water was not considered, daily P_{HMS} was generally calculated to be one to two orders of magnitude lower (**Figure S9b**) and slower P_{HMS} were determined under hazy days ($1.2 \pm 1.7 \times 10^{-4} \mu\text{g m}^{-3} \text{h}^{-1}$) compared to clean periods ($3.2 \pm 5.4 \times 10^{-4} \mu\text{g m}^{-3} \text{h}^{-1}$) (**Figure S9c**), failing to explain the observed higher HMS/CO ratio. We have also quantified the relative variations in HMS formation rate during hazy days compared to clean days ($\Delta P/P_{\text{HMS, clean}}$) corresponding to changes in SO_2 level, HCHO level, temperature, aerosol liquid water content (ALWC), aerosol pH and ionic strength. And it can be seen that even with a 4-fold increase in ALWC coupled with a 2-fold increase in HCHO levels (**Table S1**, attached below), these factors cannot completely counterbalance the potential 10-fold reduction in HMS formation rates resulting from the decreased aerosol pH and it was the reduction in aerosol ionic strength on polluted days which exhibited more pronounced enhancement in HMS formation, ultimately leading to a nearly 10-fold rise in P_{HMS} during haze episode compared to dry and clean days (**Figure S9d**). Taken together, these findings underscore the pivotal role of aerosol ionic strength in influencing HMS formation in our study.

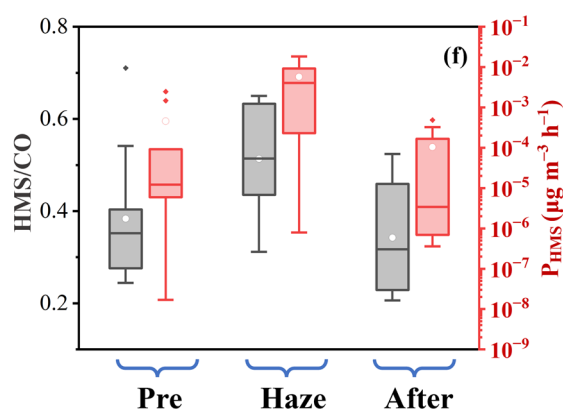


Figure 2f. Comparison between HMS/CO ratio and HMS formation rates (P_{HMS}).

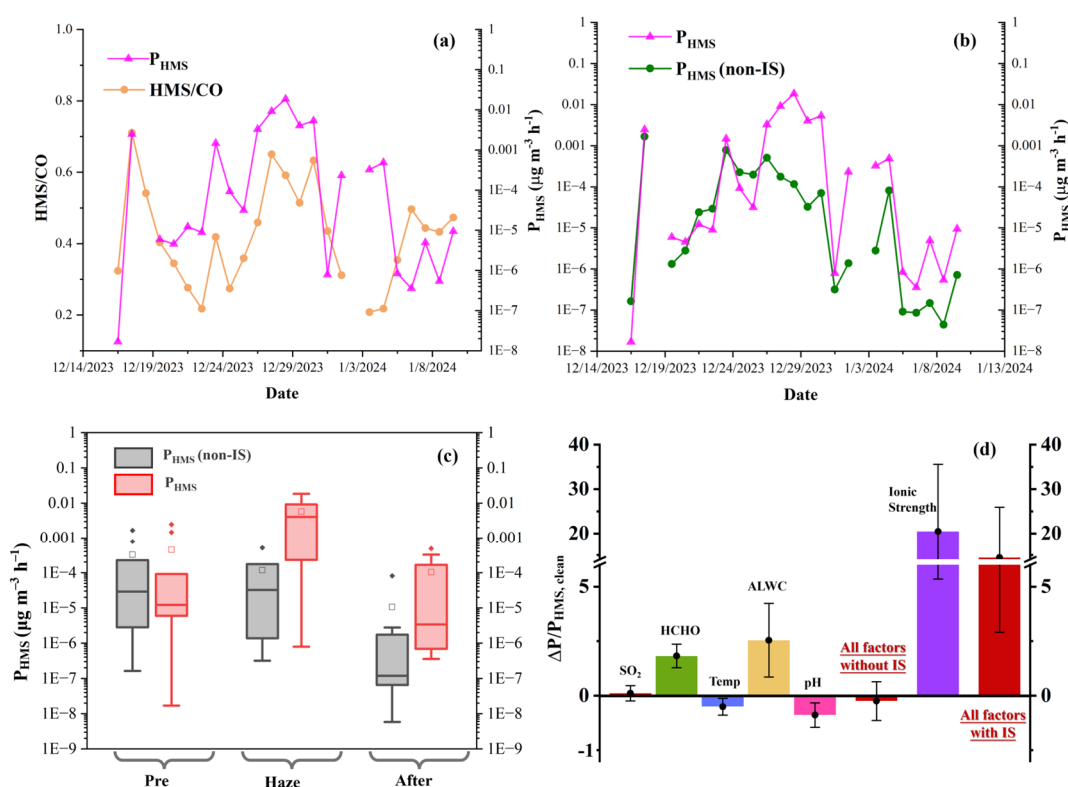


Figure S9. (a) The comparison between estimated HMS formation rate (P_{HMS}) with HMS/CO ratio in urban Nanjing; (b) The comparison between HMS/CO ratio and P_{HMS} without considering the IS effect in urban Nanjing; (c) the averaged P_{HMS} before, within and after haze event, with and without consideration of ionic strength. The formation rate estimations on December 19th, 2023 and January 3rd, 2024 are not feasible due to the absence of HCHO level and aerosol properties, respectively; (d) The relative variation in HMS formation rate during hazy days ($\Delta P/P_{HMS, \text{clean}}$) corresponding to changes in SO_2 level, HCHO level, temperature, ALWC, pH and ionic strength compared to clean days.

Table S1. Summary of atmospheric measurements in this study.

	Continental aerosol			Marine aerosol
	Pre-haze	Haze event	After haze	
T (K)	272±2 ^a	277±4	277±1	283±1
RH	52±17%	74±8%	69±5%	83±6%
PM _{2.5} (μg m ⁻³)	38.65±15.66	114.29±18.01	73.27±33.32	- ^b
SO ₂ (ppb)	1.99±0.45	2.21±0.69	2.18±0.54	0.82±0.42
HCHO (ppb)	1.91±1.05	5.38 ±1.08	3.67±0.68	-
HMS (μg m ⁻³)	0.23±0.08	0.36±0.09	0.32±0.08	0.050±0.012
Sulfate (μg m ⁻³)	4.18±1.71	11.44±4.07	8.87±4.05	2.09±0.46
HMS/Sulfate (%)	5.87±1.70%	3.36±0.73%	4.15±1.40%	2.57±0.09%
ALWC (μg m ⁻³)	22.69±20.65	80.45±38.40	61.30±36.34	14.72±6.40
pH	5.25±0.42	4.76±0.46	3.95±0.53	4.24±0.15
Ionic strength (mol kg ⁻¹)	12.32±3.19	8.85±1.30	10.39±0.85	4.30±1.24
P _{HMS} (× 10 ⁻⁴ μg m ⁻³ h ⁻¹)	4.54±8.4	57.6±58.7	1.18±1.87	0.26 ^c
HMS/CO	0.38±0.14	0.51±0.11	0.35±0.12	-

^a The numerical representation of average ± one standard deviation.

^b The data was not available.

^c The formation rate was calculated using averaged values listed above assuming the HCHO level of 0.5 ppb (Wagner et al., 2001; Anderson et al., 2017).

In addition, we have revised the caption of **Figure S1** in accordance with the guidance provided by the editorial office. We would like to express our gratitude to the editor again for your attention to our work!

Best regards,

Rongshuang XU

School of Ecology and Applied Meteorology,

Nanjing University of Information Science & Technology

Email: rongs_xu@nuist.edu.cn

References:

- Anderson, D. C., Nicely, J. M., Wolfe, G. M., Hanisco, T. F., Salawitch, R. J., Canty, T. P., Dickerson, R. R., Apel, E. C., Baidar, S., Bannan, T. J., Blake, N. J., Chen, D., Dix, B., Fernandez, R. P., Hall, S. R., Hornbrook, R. S., Gregory Huey, L., Josse, B., Jöckel, P., Kinnison, D. E., Koenig, T. K., Le Breton, M., Marécal, V., Morgenstern, O., Oman, L. D., Pan, L. L., Percival, C., Plummer, D., Revell, L. E., Rozanov, E., Saiz-Lopez, A., Stenke, A., Sudo, K., Tilmes, S., Ullmann, K., Volkamer, R., Weinheimer, A. J. and Zeng, G.: Formaldehyde in the Tropical Western Pacific: Chemical Sources and Sinks, Convective Transport, and Representation in CAM-Chem and the CCM1 Models, *Journal of Geophysical Research: Atmospheres*, **122**(20): 11,201-211,226, <https://doi.org/10.1002/2016JD026121>, 2017.
- Gelaro, R., McCarty, W., Suárez, M. J., Todling, R., Molod, A., Takacs, L., Randles, C., Darmenov, A., Bosilovich, M. G., Reichle, R., Wargan, K., Coy, L., Cullather, R., Draper, C., Akella, S., Buchard, V., Conaty, A., da Silva, A., Gu, W., Kim, G. K., Koster, R., Lucchesi, R., Merkova, D., Nielsen, J. E., Partyka, G., Pawson, S., Putman, W., Rienecker, M., Schubert, S. D., Sienkiewicz, M. and Zhao, B.: The Modern-Era Retrospective Analysis for Research and Applications, Version 2 (MERRA-2), *J Clim*, **Volume 30**(Iss 13): 5419-5454, 10.1175/jcli-d-16-0758.1, 2017.
- Herrmann, H., Schaefer, T., Tilgner, A., Styler, S. A., Weller, C., Teich, M. and Otto, T.: Tropospheric aqueous-phase chemistry: kinetics, mechanisms, and its coupling to a changing gas phase, *Chem Rev*, **115**(10): 4259-4334, 10.1021/cr500447k, 2015.
- Li, J., Wang, X., Chen, J., Zhu, C., Li, W., Li, C., Liu, L., Xu, C., Wen, L., Xue, L., Wang, W., Ding, A. and Herrmann, H.: Chemical composition and droplet size distribution of cloud at the summit of Mount Tai, China, *Atmos. Chem. Phys.*, **17**(16): 9885-9896, 10.5194/acp-17-9885-2017, 2017.
- Ma, T., Furutani, H., Duan, F., Kimoto, T., Jiang, J., Zhang, Q., Xu, X., Wang, Y., Gao, J., Geng, G., Li, M., Song, S., Ma, Y., Che, F., Wang, J., Zhu, L., Huang, T., Toyoda, M. and He, K.: Contribution of hydroxymethanesulfonate (HMS) to severe winter haze in the North China Plain, *Atmospheric Chemistry and Physics*, **20**(10): 5887-5897, 10.5194/acp-20-5887-2020, 2020.
- Shah, V., Jacob, D. J., Moch, J. M., Wang, X. and Zhai, S.: Global modeling of cloud water acidity, precipitation acidity, and acid inputs to ecosystems, *Atmos. Chem. Phys.*, **20**(20): 12223-12245, 10.5194/acp-20-12223-2020, 2020.
- Song, S., Gao, M., Xu, W., Sun, Y., Worsnop, D. R., Jayne, J. T., Zhang, Y., Zhu, L., Li, M., Zhou, Z., Cheng, C., Lv, Y., Wang, Y., Peng, W., Xu, X., Lin, N., Wang, Y., Wang, S., Munger, J. W., Jacob, D. J. and McElroy, M. B.: Possible heterogeneous chemistry of hydroxymethanesulfonate (HMS) in northern China winter haze, *Atmospheric Chemistry and Physics*, **19**(2): 1357-1371, 10.5194/acp-19-1357-2019, 2019.
- Wagner, V., Schiller, C. and Fischer, H.: Formaldehyde measurements in the marine boundary layer of the Indian Ocean during the 1999 INDOEX cruise of the R/V Ronald H. Brown, *Journal of Geophysical Research: Atmospheres*, **106**(D22): 28529-28538, 10.1029/2000jd900825, 2001.
- Wang, H., Li, J., Wu, T., Ma, T., Wei, L., Zhang, H., Yang, X., Munger, J. W., Duan, F. K., Zhang, Y., Feng, Y., Zhang, Q., Sun, Y., Fu, P., McElroy, M. B. and Song, S.: Model Simulations and Predictions of Hydroxymethanesulfonate (HMS) in the Beijing-Tianjin-Hebei Region,

China: Roles of Aqueous Aerosols and Atmospheric Acidity, *Environ Sci Technol*, **58**(3): 1589-1600, 10.1021/acs.est.3c07306, 2024.

Wang, T., Liu, M., Liu, M., Song, Y., Xu, Z., Shang, F., Huang, X., Liao, W., Wang, W., Ge, M., Cao, J., Hu, J., Tang, G., Pan, Y., Hu, M. and Zhu, T.: Sulfate Formation Apportionment during Winter Haze Events in North China, *Environmental Science & Technology*, **56**(12): 7771-7778, 10.1021/acs.est.2c02533, 2022.

Wei, L., Fu, P., Chen, X., An, N., Yue, S., Ren, H., Zhao, W., Xie, Q., Sun, Y., Zhu, Q.-F., Wang, Z. and Feng, Y.-Q.: Quantitative Determination of Hydroxymethanesulfonate (HMS) Using Ion Chromatography and UHPLC-LTQ-Orbitrap Mass Spectrometry: A Missing Source of Sulfur during Haze Episodes in Beijing, *Environmental Science & Technology Letters*, **7**(10): 701-707, 10.1021/acs.estlett.0c00528, 2020.

Williams, A. G., Chambers, S. D., Conen, F., Reimann, S., Hill, M., Griffiths, A. D. and Crawford, J.: Radon as a tracer of atmospheric influences on traffic-related air pollution in a small inland city, *Tellus B: Chemical and Physical Meteorology*, **68**(1), 10.3402/tellusb.v68.30967, 2016.